



Classifying Colorectal Cancer by Tumor Location Rather than Sidedness Highlights a Continuum in Mutation Profiles and Consensus Molecular Subtypes

Jonathan M. Loree¹, Allan A.L. Pereira¹, Michael Lam¹, Alexandra N. Willauer¹, Kanwal Raghav¹, Arvind Dasari¹, Van. K Morris¹, Shailesh Advani¹, David G. Menter¹, Cathy Eng¹, Kenna Shaw², Russell Broaddus³, Mark J. Routbort⁴, Yusha Liu⁵, Jeffrey S. Morris⁵, Rajyalakshmi Luthra⁴, Funda Meric-Bernstam⁶, Michael J. Overman¹, Dipen Maru³, and Scott Kopetz¹

Abstract

Purpose: Colorectal cancers are classified as right/left-sided based on whether they occur before/after the splenic flexure, with established differences in molecular subtypes and outcomes. However, it is unclear if this division is optimal and whether precise tumor location provides further information.

Experimental Design: In 1,876 patients with colorectal cancer, we compared mutation prevalence and overall survival (OS) according to side and location. Consensus molecular subtype (CMS) was compared in a separate cohort of 608 patients.

Results: Mutation prevalence differed by side and location for *TP53*, *KRAS*, *BRAFV600*, *PIK3CA*, *SMAD4*, *CTNNB1*, *GNAS*, and *PTEN*. Within left- and right-sided tumors, there remained substantial variations in mutation rates. For example, within right-sided tumors, *RAS* mutations decreased from 70% for cecal, to 43% for hepatic flexure location ($P = 0.0001$), while *BRAFV600* mutations increased from 10% to 22%

between the same locations ($P < 0.0001$). Within left-sided tumors, the sigmoid and rectal region had more *TP53* mutations ($P = 0.027$), less *PIK3CA* ($P = 0.0009$), *BRAF* ($P = 0.0033$), or *CTNNB1* mutations ($P < 0.0001$), and less MSI ($P < 0.0001$) than other left-sided locations. Despite this, a left/right division preceding the transverse colon maximized prognostic differences by side and transverse colon tumors had K-modes mutation clustering that appeared more left than right sided. CMS profiles showed a decline in CMS1 and CMS3 and rise in CMS2 prevalence moving distally.

Conclusions: Current right/left classifications may not fully recapitulate regional variations in tumor biology. Specifically, the sigmoid-rectal region appears unique and the transverse colon is distinct from other right-sided locations. *Clin Cancer Res*; 24(5); 1062–72. ©2017 AACR.

See related commentary by Dienstmann, p. 989

Introduction

Primary tumor sidedness has prognostic value in metastatic colorectal cancer (mCRC). Patients with right-sided tumors have worse overall survival (OS) following first-line chemotherapy than those with left-sided tumors (1). This effect appears inde-

pendent of *BRAF* mutation status and mucinous histology, both of which are more common in right-sided tumors (2). There are other molecular features that distinguish right- from left-sided tumors, including a higher incidence of microsatellite instability (MSI), an association with CpG island methylator phenotype (CIMP-H), and an association with consensus molecular subtype-1 (CMS-1) in right-sided tumors (3–5). Each of these features is individually associated with worse outcomes; however, when analyzed in multivariate models that control for these factors, it appears that tumor location is still important (3, 6). This suggests that we do not fully understand the molecular underpinnings of this phenomenon.

Retrospective analyses of multiple trials have shown that in *RAS/BRAF* wild-type patients with mCRC, there is a differential response to anti-EGFR therapy based on side (7, 8). In CRYSTAL, FIRE-3, PRIME, PEAK, 80405, 181, and NCIC CO.17, it appeared that left-sided tumors have improved outcomes with anti-EGFR therapy, while right-sided tumors have a worse outcome than if they did not receive anti-EGFR therapy (9–13). This differential outcome by side was not only present, but was very large. In 80405, median OS (mOS) for right-sided patients treated with a doublet + bevacizumab was 29.2 months, compared with 13.7 months with a doublet + cetuximab. This stands in stark contrast

¹Gastrointestinal Medical Oncology, The University of Texas MD Anderson Cancer Center, Houston, Texas. ²Sheikh Khalifa Bin Zayed Al Nahyan Institute of Personalized Cancer Therapy, The University of Texas MD Anderson Cancer Center, Houston, Texas. ³Department of Pathology, The University of Texas MD Anderson Cancer Center, Houston, Texas. ⁴Department of Hematopathology, The University of Texas MD Anderson Cancer Center, Houston, Texas. ⁵Department of Biostatistics, The University of Texas MD Anderson Cancer Center, Houston, Texas. ⁶Investigational Cancer Therapeutics, The University of Texas MD Anderson Cancer Center, Houston, Texas.

Note: Supplementary data for this article are available at Clinical Cancer Research Online (<http://clincancerres.aacrjournals.org/>).

Corresponding Author: Scott Kopetz, The University of Texas MD Anderson Cancer Center, Unit 426, 1515 Holcombe Blvd, Houston, TX 77030. Phone: 713-792-2828; Fax: 713-563-6764; E-mail: skopetz@mdanderson.org

doi: 10.1158/1078-0432.CCR-17-2484

©2017 American Association for Cancer Research.

Translational Relevance

Primary tumor sidedness is prognostic in metastatic colorectal cancer, with right-sided tumors having a worse prognosis than left-sided tumors even after controlling for known negative prognostic factors such as *BRAF* mutations that differ between right- and left-sided tumors. Recent analysis suggests that sidedness may also be a predictive marker for response to anti-EGFR therapy. In *RAS* wild-type patients, left-sided tumors appear to derive benefit from anti-EGFR therapy, while right-sided tumors do not. The molecular underpinnings of this differential response are currently unclear. Here, we present the mutational and molecular subtype profiles divided by the previously established left versus right division as well as by unique colonic location. We demonstrate that these profiles vary dramatically throughout the colon and that a simple left versus right divide may be oversimplifying the geographically distinct biology present in colorectal cancer.

to an mOS of 39.3 months for doublet + cetuximab versus 32.7 months for doublet + bevacizumab in left-sided tumors (11). In a meta-analysis that included the data from all of these trials, left-sided patients were shown to have greater benefit from chemotherapy + anti-EGFR (HR, 0.71; 95% CI, 0.58–0.85; $P = 0.0003$) compared with chemotherapy + bevacizumab, while right-sided tumors had trends toward harm with anti-EGFR therapy (HR, 1.3; 95% CI, 0.97–1.74; $P = 0.081$; ref. 1).

Given that disparate responses to anti-EGFR therapy based on side were present in *RAS/BRAF* wild-type patients, it is clear that further assessment of the biological differences between tumors at different locations is required. Until now, most studies have used a divide of the splenic flexure to split right/proximal tumors from left/distal tumors. We sought to evaluate whether a more precise definition of tumor location may provide further information about a tumor's biology and clinical course. We retrospectively reviewed all clinical and next-generation sequencing (NGS) panel data from 1,876 patients with mCRC and have summarized the molecular alterations based on tumor location with the typical left versus right division, as well as by the anatomic sites of cecum, ascending colon, hepatic flexure, transverse colon, splenic flexure, descending colon, sigmoid colon, rectosigmoid junction, and rectum. We also present a comparison of OS based on location subsite. In two additional cohorts, CMS subtype and CpG island methylator phenotype have been compared by side and location.

Patients and Methods

Patient population

After obtaining approval from the institutional review board at The University of Texas MD Anderson Cancer Center (MDACC), the records of all patients with biopsy proven mCRC who had a 46 or 50 gene Clinical Laboratory Improvement Amendments (CLIA) NGS panel performed as part of their care between January 1, 2012, and September 1, 2016, were reviewed. Right-sided tumors were defined based on pathology and surgical reports as those occurring from the cecum up to but not including the splenic flexure, while left-sided colon cancers were defined as occurring from the splenic flexure to the rectum. The pathology department uses a mixture of information from the specimen

label submitted by a surgeon, type of surgery, and measurement of distance from known anatomic landmarks or proximal and distal margins to assign a tumor location. For endoscopically defined locations, the annotation of location from the endoscopy report is used for annotation. For patients with resection performed outside of MD Anderson, a pathology review is obtained on any available primary resection specimens or tissue biopsies, and surgical or endoscopic reports are reviewed. This information is collected in a uniform manner by our tumor registry as part of the institution's NCI Cancer Center Support Grant. After primary review of tumor location, the primary coder then gives the chart to a second coder who verifies site, histology and stage. Through this process, we are able to provide two-coder verification for all charts abstracted. In more difficult cases, the manager of the coding section will contact colorectal cancer physicians to assure that the most accurate information is abstracted.

A second cohort of 196 patients from MDACC with Affymetrix microarray RNA expression was combined with 412 patients from The Cancer Genome Atlas (TCGA) project with publicly available expression data to compare CMS subtype by location (14). Patients in this second cohort were stage I to IV, and this population was utilized only for comparison of CMS subtype distribution by location. A previously published gene expression profile was used for this classification (4). A third cohort of 457 mCRC patients was reviewed to provide information about CpG island methylation phenotype status. These patients were derived from the ATTACC umbrella protocol (NCT01196130) at MDACC. PCR-based pyrosequencing of DNA was performed to examine the methylation status of multiple CpG island loci for each of the tested genes (*hMLH1*, *Mint1*, *Mint2*, *Mint31*, *p14*, and *p16*). CIMP-H tumors were defined as those with $\geq 40\%$ of CpG Island loci methylated.

NGS panel

Tumor sequencing was performed in the CLIA environment of MDACC's Molecular Diagnostics Laboratory. Archival formalin-fixed paraffin embedded (FFPE) samples from either surgical resection specimens or tissue biopsies with $>20\%$ tumor content were used for sequencing. Sequencing results from primaries or metastatic biopsies were considered together as prior evidence suggests there is a high level of concordance between primary and metastatic lesions (15). DNA extraction used a PicoPure DNA extraction kit (Arcturus) and was purified using an Agencourt AMPure XP kit (Agencourt Biosciences). DNA quantification was performed with a Qubit DNA assay kit (ThermoFisher Scientific). Library preparation was performed using the Ion Torrent AmpliSeq 2.0 Beta kit and Ion Torrent AmpliSeq Cancer Panel Primers (Life Technologies). Until September 10, 2013, version 1.0 of the panel which included 46 cancer-related genes was utilized. Subsequently, version 2.0 of the panel was used which included an additional 4 genes. For patients who had version 2.0, only the 46 genes used for the entire cohort were reported. Sequencing was performed using an Ion Torrent Personal Genome Machine Sequencer and adequately covered amplicons were defined as those having a coverage depth of ≥ 250 reads. The lower limit of detection of this assay is between 5% and 10%. Sequence alignment and base calling were performed using the Torrent Suite software version 2.01 and variant calling was performed with Torrent Variant Caller software version 1.0 with Human Genome Build 19 as the reference. Routine germ line testing was not performed. Tested codons and genes have been previously described (16).

Loree et al.

MSI testing

MSI status was retrospectively reviewed from patient's charts and was evaluated only in patients who had testing performed as part of their clinical care. This consisted of a mixture of immunohistochemistry for mismatch repair protein deficiency and PCR based assessment of microsatellite status. Tumors were defined as MSI-H if either method of detection was abnormal.

Statistical methods

Differences in mutation rates for each gene and categorical baseline characteristics were compared using the χ^2 test, while an ANOVA was used to compare age. In the analysis of mutation prevalence, a χ^2 test was performed across all sites (global P in Supplementary Table S1) and a repeat analysis was performed in only those tumors defined as right or left sided (right/left P in Supplementary Table S1) to determine if there was significant variance in mutation rates across sites of the same side. Rectal tumors were considered separately in analyses based on tumor side. By modeling the relative location as semicontinuous, a generalized additive model was used to generate a prevalence estimates by location (Figs. 1 and 3). In order to assess whether transverse colon tumors were more similar to right- or left-sided tumors, we performed K-modes clustering. A K-modes clustering algorithm was applied rather than a K-means or hierarchical clustering as mutational data were categorical. K-modes clustering is specifically designed for categorical data where standard distance matrices may not be applicable (17–19). K-modes clustering used an unweighted algorithm with a maximum of 10-iterations and patients were clustered into 2 clusters. All available mutation data from the 46 genes were utilized. A sensitivity analysis was performed with a subset of 10 genes that were either commonly altered or clinically relevant; however, this did not alter the results.

OS was defined as the interval from diagnosis with mCRC to date of death from any cause. Patients alive at the time of last follow-up were censored. Cox regression models were used to compare OS by tumor location and multivariate Cox proportional hazard models were generated for OS using location and any variable that differed by side or site in Tables 1, 2, or Supplemental Table S1 entered into the model using a forward likelihood ratio selection with $P < 0.1$ for inclusion of variables. All variables met the proportional hazards assumption except gender, which was used as a stratification factor for the analysis. For survival analysis, the tumor location of rectum was considered the reference as it could remain consistent between analyses based on both side and location, and because it represented the largest group of patients, making it statistically robust. A two-sided P value of <0.05 was considered significant. Analysis was performed with GraphPad Prism software version 5.0, SPSS version 22.0, and R studio version 3.30. K-modes clustering was performed using the *klar* package (20). Graphical presentation of data also used Tableau version 10.1 and ggplot2 (21).

Results

Baseline characteristics

Information regarding tumor side was available for the entire cohort, while 51 of 1,876 patients lacked enough information to define the exact location of a primary tumor. Table 1 summarizes baseline characteristics stratified by both tumor side and location. Median age, MSI status, synchronous versus metachronous pre-

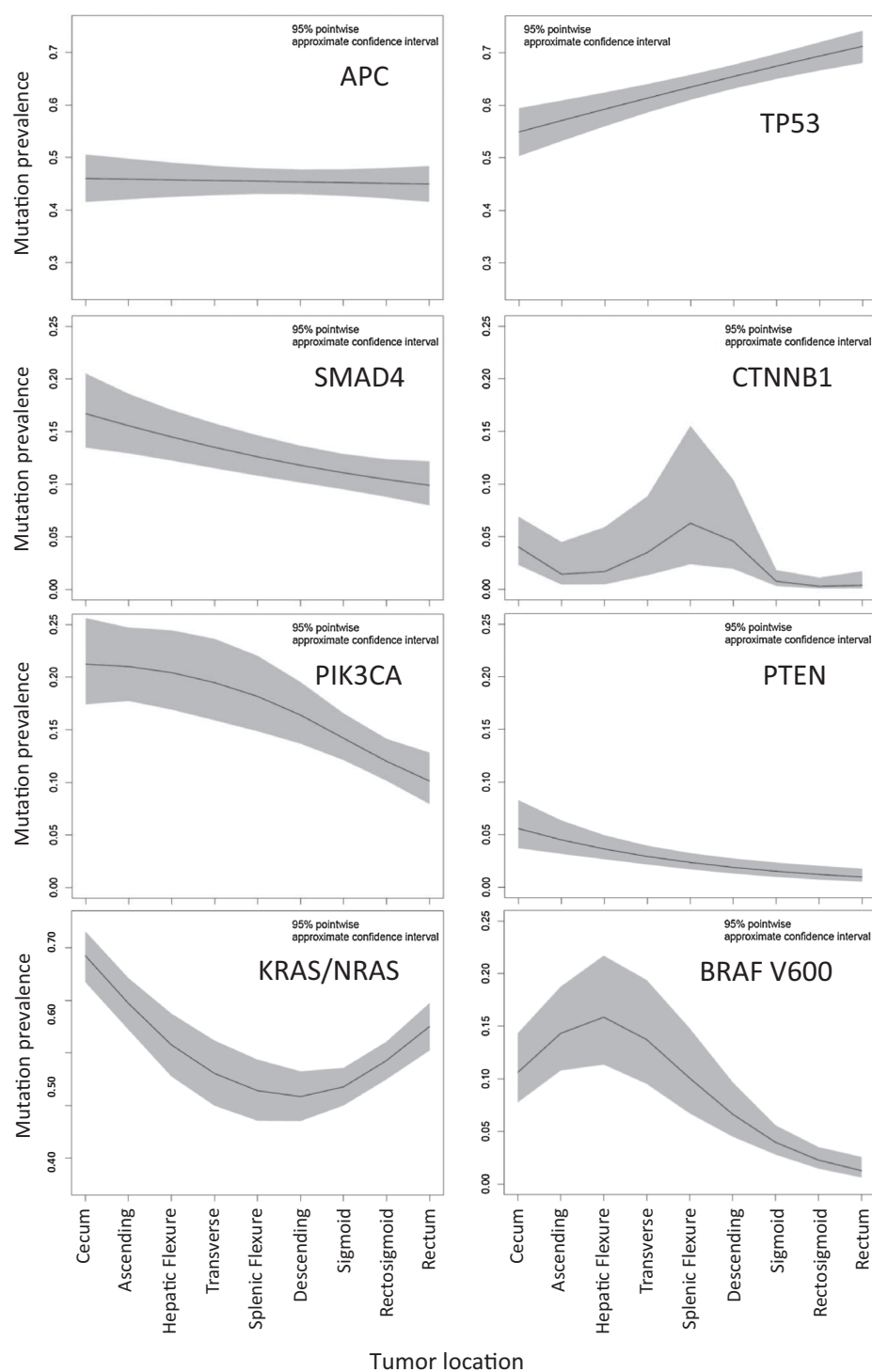
sentation, and histology all differed by both side and location, while gender was only significantly different when comparing tumors by side. Patients with right-sided tumors were older ($P < 0.0001$), more likely to present with synchronous metastatic disease ($P < 0.0001$), and more likely to have mucinous histology (27%) than left-sided (15%) or rectal tumors (9%; $P < 0.0001$). Men made up a larger proportion of patients with left-sided (58%) and rectal (61%), than right-sided tumors (51%; $P = 0.002$). Similar directionality and trends for age ($P < 0.0001$), gender ratio ($P = 0.058$), and synchronous versus metachronous disease presentation ($P = 0.001$) were noted based on location. Signet/mucinous histology differed by locations located within the same side of the colon. This histology was highest in the cecum (29%) and gradually fell moving distally, with a second peak in the descending colon (24%), which was notably higher than the prevalence in the splenic flexure (16%) or transverse colon (16%; $P < 0.0001$). MSI status rose from the cecum (5%) to the ascending colon (10%) and hepatic flexure (12%) before gradually decreasing through the rest of the colon ($P < 0.0001$).

Molecular profile

TP53, *KRAS*, *PIK3CA*, *SMAD4*, *BRAFV600*, *PTEN*, *CTNNB1*, and *GNAS* mutation prevalence all differed by both side and location, while *FGFR3* only differed by side (Table 2 and Supplementary Table S1). When a Bonferroni correction was applied, *TP53*, *KRAS*, *PIK3CA*, *BRAFV600*, *PTEN*, and *GNAS* remained significant by side ($P < 0.002$), while *TP53*, *KRAS*, *PIK3CA*, *BRAFV600* and *CTNNB1* remained significant by location ($P < 0.002$). Prevalence estimates did not vary considerably based on whether the sequenced biopsy was from a primary tumor or metastatic lesion that had spread from the same site (Supplementary Fig. S1). Overall, 62% of results were from a primary, while 38% of results came from a biopsy of a metastasis. Liver (51%), lung (17%), and gynecological (7%) were the most common sites for biopsies. Only genes with mutations present in >10 of the 1,876 patients are reported in Tabular format, while Fig. 1 presents key genes in colorectal oncology graphed using a generalized additive model to provide point estimates of mutation prevalence with 95% CI. *KRAS* and *NRAS* have been graphed together. Rates of *TP53* mutations rise moving distally, while *PIK3CA*, *BRAFV600*, and *SMAD4* mutations fall in prevalence. Exceptions to this include elevated *PIK3CA* (26%, $P = 0.0009$) and *BRAFV600* (9%, $P = 0.0033$) mutation rates in the descending colon compared with other left-sided tumor locations and higher *CTNNB1* mutation rates at the splenic flexure (6%) and descending colon (6%) compared with other left-sided locations ($P < 0.0001$). *KRAS* mutations fall moving right to left, but then rise again in the rectum, while *NRAS* mutations appear absent from the area between the hepatic flexure and descending colon, though this was not significant ($P = 0.24$).

As seen in Fig. 1 and Supplemental Table S1, mutation prevalence varies dramatically within tumors of the same side but at different locations. Notable examples include (i) *RAS* mutations are seen in 70% of cecal tumors but only 57% of ascending colon and 43% of hepatic flexure tumors ($P = 0.0008$), (ii) *BRAFV600* mutations occur in 10% of cecal, 16% of ascending colon, and 22% of hepatic flexure tumors ($P < 0.0001$), (iii) *PIK3CA* mutations are seen in 26% of descending colon but only 14% of sigmoid and 9% of rectosigmoid tumors ($P = 0.0009$), and (iv) *CTNNB1* mutations are almost absent in the sigmoid (1%),

Figure 1.
Relative prevalence of key oncogenic alterations at specific primary tumor locations in patients with metastatic colorectal cancer.

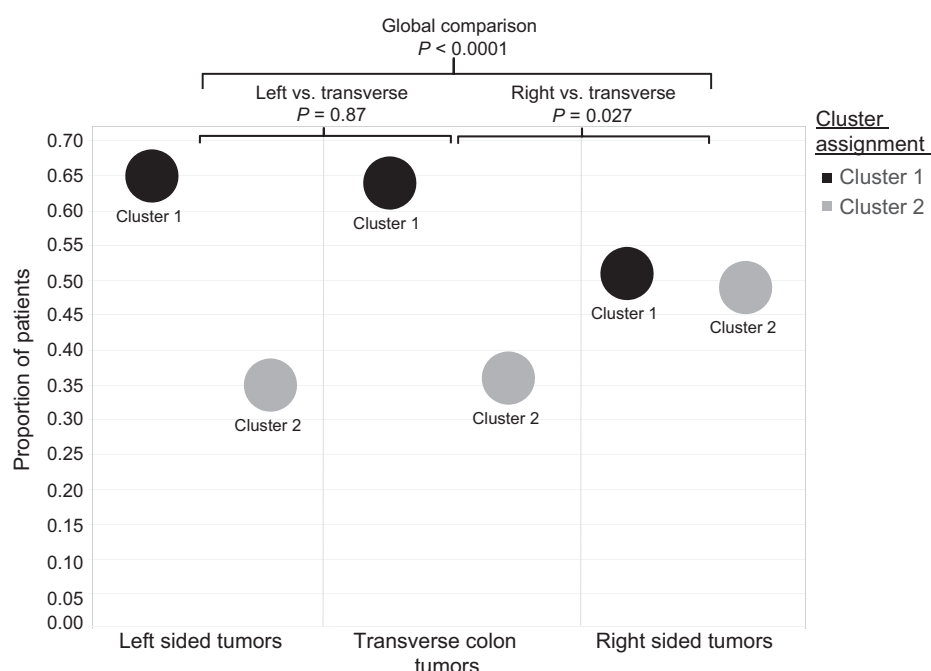


rectosigmoid junction (0%), and rectum (1%), but are still present in the descending colon (6%; $P < 0.0001$).

Relative prevalence of mutation clusters identified using K-modes clustering differed significantly based on tumor location ($P < 0.0001$). When the mutation clusters of cecum, ascending colon, hepatic flexure, and transverse colon were compared with each other, strong trends toward differing cluster prevalence

($P = 0.056$) existed among these right-sided locations. When mutation clusters of splenic flexure, descending colon, sigmoid colon, rectosigmoid colon, and rectum were compared, they did not differ ($P = 0.26$). Given the noted differences among right-sided locations, we directly compared transverse colon tumors to left- and right-sided tumors (excluding transverse) to see if it appeared more right or left sided. Transverse colon tumors

Loree et al.

**Figure 2.**

K-mode clustering of mutational profiles of metastatic colorectal cancers classified by tumor location to help establish an optimal right versus left cut point. Each cluster represents a distinct group of mutations that either commonly co-occur or are mutually exclusive and are used for grouping similar patients together.

differed from right-sided ($P = 0.027$) but not left-sided ($P = 0.87$) locations (Fig. 2) in K-modes clustering.

To ensure that k-modes clustering results were robust for methodology, we analyzed the samples with different approaches. Because many of the mutations will not be present in most patients, we chose the 10 most common or clinically relevant mutations and repeated the analysis to help address the question of whether co-occurring or mutually exclusive alterations may be affecting our results. Genes included were *TP53*, *APC*, *FBXW7*, *SMAD4*, *PIK3CA*, *ATM*, *PTEN*, *KRAS*, *NRAS*, and *BRAF*. Clustering was identical to the main analysis. Subsequently, we also repeated the clustering with a "leave one out" strategy where we repeated the clustering with 9 of the 10 most common alterations, each time leaving out one of the alterations. If *APC* ($P = 0.032$), *PTEN* ($P = 0.027$), *TP53* ($P = 0.068$), *PIK3CA* ($P = 0.067$), or *KRAS* ($P = 0.15$) were left out of clustering, a similar difference between cluster prevalence was noted between right and transverse colon tumors, but not left-sided lesions. All other potential combinations did not reveal statistically different mutation clusters between transverse tumors and either right- or left-sided tumors.

CpG island methylator status

CIMP data were available for a separate cohort of 457 mCRC patients and demonstrated significantly higher rates of CIMP-H phenotype among right-sided tumors (29%) than left-sided (17%) or rectal (23%) tumors ($P = 0.028$). There were no statistically significant differences among tumor locations that are traditionally grouped on the same side (Table 2 and Supplementary Table S1).

CMS distribution

We noted increasing rates of CMS2 moving from right to left, accompanied by a fall in CMS1, while CMS3 and CMS4 were relatively stable when we compared CMS by tumor side (Table 2). When comparing CMS subtype by location (Fig. 3 and Supple-

mentary Table S1), CMS1 rises from the cecum (29%) to the ascending colon (41%) and hepatic flexure (52%) before falling throughout the rest of the colon. CMS2 shows a general increase moving distally from the cecum (28%), with a peak in the sigmoid (65%) and rectosigmoid regions (65%). CMS3 shows a gradual decrease moving distally, while CMS4 stays relatively stable outside of an increased prevalence in the descending colon (43%). The relative proportion of individual subtypes was significantly different based on both side ($P < 0.0001$) and location ($P < 0.0001$; Table 2 and Supplementary Table S1).

Survival analysis

With a median follow-up time of 46.5 months, we noted that right-sided tumors are associated with a worse OS (HR, 1.63; 95% CI, 1.38–1.89, $P < 0.0001$) than left-sided (HR, 0.98; 95% CI, 0.84–1.16, $P = 0.84$) or rectal tumors (reference). Figure 4A demonstrates the relative impact of tumor location on the hazard ratio for OS compared with rectal tumors as the reference group. With increased granularity in localization, cecal (HR, 1.69; 95% CI, 1.40–2.04, $P < 0.0001$), ascending colon (HR, 1.72; 95% CI, 1.34–2.21, $P < 0.0001$), hepatic flexure (HR, 1.98; 95% CI, 1.38–2.85, $P < 0.0001$), and transverse colon (HR, 1.38; 95% CI, 1.02–1.88, $P = 0.038$) tumors all appeared associated with a worse prognosis than left-sided or rectal tumors. We performed a sensitivity analysis to assess whether different geographic cut-points between right- and left-sided tumors could be found that maximized the HR between sides (Supplementary Fig. S2) and noted that the maximum difference in HR for OS could be generated by including all locations beyond the hepatic flexure together as a "left-sided" group compared with all locations from the cecum up to and including the hepatic flexure, as a "right-sided" group.

In order to assess whether the clinicopathologic or mutation differences we noted in our study explained all of the differential prognosis based on location, we constructed multivariate models controlling for all co-variables that differed based on either side or

Table 1. Baseline characteristics of patients with colorectal cancer classified by tumor side and tumor location

	Stratified by side				Stratified by tumor site								P
	Right-sided colon	Left-sided colon	Rectum	P	Cecum	Ascending colon	Hepatic flexure	Transverse colon	Splenic flexure	Descending colon	Sigmoid colon	Rectosigmoid junction	Rectum
Number	604 (32)	850 (45)	422 (23)		313 (17)	124 (7)	51 (3)	86 (5)	36 (2)	78 (4)	521 (29)	194 (11)	422 (23)
Median age (IQR)	57 (49–65)	53 (44–61)	54 (45–62)	<0.0001	58 (49–65)	57 (49–64)	58 (50–65)	56 (48–65)	54 (45–63)	53 (41–63)	53 (43–60)	52 (45–60)	54 (45–62)
Gender													
Female	298 (49)	355 (42)	165 (39)	0.002	156 (50)	63 (51)	23 (45)	43 (50)	14 (39)	29 (37)	217 (42)	87 (45)	165 (39)
Male	306 (51)	495 (58)	257 (61)		157 (50)	61 (49)	28 (55)	43 (50)	22 (61)	49 (63)	304 (58)	107 (55)	257 (61)
MSI status ^a													
Stable	447 (93)	680 (98)	340 (98)	<0.0001	240 (95)	88 (90)	38 (88)	63 (94)	26 (93)	63 (96)	422 (98)	156 (99)	340 (98)
Unstable	33 (7)	16 (2)	8 (2)		12 (5)	10 (10)	5 (12)	4 (6)	2 (7)	3 (5)	10 (2)	1 (1)	8 (2)
Stage IV diagnosis													
Synchronous	416 (69)	565 (67)	233 (55)	<0.0001	218 (70)	83 (67)	37 (73)	60 (70)	26 (73)	48 (62)	354 (68)	127 (66)	233 (55)
Metachronous	188 (31)	285 (34)	189 (45)		95 (30)	41 (33)	14 (27)	26 (30)	10 (28)	30 (39)	167 (32)	67 (35)	189 (45)
Histology													
Adenocarcinoma	438 (73)	724 (85)	386 (92)	<0.0001	219 (70)	90 (73)	39 (77)	72 (84)	33 (92)	58 (74)	446 (86)	171 (88)	386 (92)
Signet/mucinous	163 (27)	123 (15)	36 (9)		92 (29)	33 (27)	12 (24)	14 (16)	3 (8)	19 (24)	73 (14)	23 (12)	36 (9)
Other	3 (1)	0 (0)	3 (0)		2 (1)	1 (1)	0 (0)	0 (0)	0 (0)	1 (1)	2 (0)	0 (0)	0 (0)
Median follow-up time (months)	49.9	46.1	44.4		47.5	52.6	47.9	43.9	48.9	50.1	47.6	43.2	44.4

NOTE: Values in the table represent the number followed in parentheses by percentage. Fifty patients did not have enough details in their operative/pathology reports to assign a tumor site, but it was possible to determine the tumor side. IQR, interquartile range. Bolded numbers are statistically significant at $P < 0.05$.

^aUnknown MSI status in 352 patients.

site in Tables 1 and 2 and Supplementary Table S1. Even after controlling for known negative prognostic markers that differed by location, right-sided tumors had a worse OS (HR, 1.35; 95% CI, 1.11–1.64, $P = 0.002$; Supplementary Fig. S3). In the model based on tumor location, the cecum (HR, 1.33; 95% CI, 1.06–1.67, $P = 0.012$), ascending colon (HR, 1.39; 95% CI, 1.03–1.87, $P = 0.029$), and the hepatic flexure (HR, 1.70; 95% CI, 1.13–2.57, $P = 0.011$) remained significantly associated with a worse OS, however the transverse colon was no longer associated with a worse OS ($P = 0.18$; Fig. 4B). When comparing transverse colon tumors to all other right-sided tumors, there was no difference in mOS in univariate (HR, 0.82; 95% CI, 0.61–1.10, $P = 0.19$) or multivariate (HR, 0.80; 95% CI, 0.60–1.08, $P = 0.15$) models. Full model details are included in Supplementary Table S3.

Given differences in transverse colon molecular profiling that suggested the transverse location differed from other right-sided locations, we assessed response to anti-EGFR therapy in RAS/*BRAF* V600 wild-type transverse colon tumors. Of 17 patients treated previously with anti-EGFR therapy in the second or later line of treatment and assessable for response, 6 (35%, 95% CI, 14%–62%) had an objective response using RECIST 1.1 criteria (22). Progression-free survival was 5.9 months, and the disease control rate was 82%. Four patients received anti-EGFR therapy in the second line, 11 in the third line, and 2 in the fourth line. All patients received anti-EGFR with a cytotoxic and 10 of them received anti-EGFR treatment with a doublet.

Discussion

We present the molecular characterization of 1,876 patients with mCRC classified by both tumor side and location. Our results highlight many previously documented differences between right/left-sided tumors. These include higher rates of *BRAF*, *PIK3CA*, *CTNNB1*, *SMAD4*, and *KRAS* mutations, higher rates of mucinous histology, higher rates of CIMP, and increased incidence of MSI among right-sided tumors, with higher rates of *TP53* mutations among left-sided tumors (23–28). Our study extends these findings to demonstrate the presence of significant differences in mutation prevalence based on tumor location that would not be noted in the classical stratification of right, left, and rectal locations. Specific alterations of note include an extremely high rate of RAS mutations in cecal primaries (70%), a rise in *BRAF*V600 mutations from the cecum (10%) to the hepatic flexure (22%), and inversely related rates of *TP53* and *APC* mutations as one moves from right to left.

Beyond suggesting that tumor location may provide more information about the biology of colorectal cancer, our results raise an important question about whether current divisions between right- and left-sided locations are optimal. The majority of recent studies assessing the impact of sidedness on response to anti-EGFR agents have divided the colon at the splenic flexure, with the exception of 80405 which excluded transverse tumors from their analysis (7, 10, 12, 13). We noted that transverse colon tumors had mutational profiles that were dissimilar from right-sided ($P < 0.0001$) but not left-sided ($P = 0.87$) tumors. Additionally, Supplemental Figure 2S demonstrates that by dividing the colon into left/right before the transverse colon we maximize the HR for our survival analysis between left/right, though there is considerable overlap of the HR confidence intervals for all locations except the rectal-sigmoid region. As well, the poor prognosis of transverse tumors noted in our univariate model, were

Loree et al.

Table 2. Mutation and consensus molecular subtype profile of patients with colorectal cancer classified by tumor side

	All patients	Right-sided colon	Left-sided colon	Rectum	P
Number	1,876	604 (32)	850 (45)	422 (23)	
TP53	1213 (65)	341 (57)	581 (68)	291 (69)	<0.0001
KRAS	909 (48)	351 (58)	343 (40)	215 (51)	<0.0001
APC	847 (45)	267 (44)	394 (46)	186 (44)	0.63
PIK3CA	287 (15)	122 (20)	121 (14)	44 (10)	<0.0001
SMAD4	233 (12)	98 (16)	87 (10)	48 (11)	0.0020
BRAF V600	115 (6)	76 (13)	34 (4)	5 (1)	<0.0001
FBXW7	142 (8)	43 (7)	58 (7)	41 (10)	0.16
NRAS	79 (4)	25 (4)	34 (4)	20 (5)	0.82
PTEN	46 (2)	29 (5)	13 (2)	4 (1)	<0.0001
ATM	41 (2)	16 (3)	17 (2)	8 (2)	0.64
CTNNB1	30 (2)	18 (3)	10 (1)	2 (1)	0.003
GNAS	30 (2)	20 (3)	8 (1)	2 (1)	<0.0001
ERBB4	22 (1)	5 (1)	10 (1)	7 (2)	0.48
ERBB2	20 (1)	5 (1)	8 (1)	7 (2)	0.40
KDR	19 (1)	5 (1)	9 (1)	5 (1)	0.84
RB1	16 (1)	7 (1)	6 (1)	3 (1)	0.61
RET	16 (1)	5 (1)	8 (1)	3 (1)	0.91
SMO	16 (1)	6 (1)	6 (1)	4 (1)	0.82
SMARCB1	15 (1)	6 (1)	6 (1)	3 (1)	0.81
AKT1	14 (1)	8 (1)	3 (1)	3 (1)	0.11
STK11	14 (1)	4 (1)	5 (1)	5 (1)	0.49
KIT	13 (1)	4 (1)	7 (1)	2 (1)	0.77
CDKN2A	12 (1)	4 (1)	4 (1)	4 (1)	0.60
MET	12 (1)	5 (1)	5 (1)	2 (1)	0.76
FGFR3	11 (1)	4 (1)	1 (0)	6 (1)	0.016
Consensus molecular subtype cohort (n = 608)					
Number	608	268	236	104	<0.0001
CMS I	104 (17)	96 (36)	6 (3)	4 (4)	
CMS II	281 (46)	77 (29)	145 (61)	58 (56)	
CMS III	78 (13)	44 (16)	20 (8)	14 (13)	
CMS IV	144 (24)	51 (19)	65 (28)	28 (27)	
CpG island methylator phenotype (CIMP) cohort (n = 457)					
Number	457	169	202	86	0.028
CIMP-H	104 (23)	49 (29)	35 (17)	20 (23)	

NOTE: Bolded numbers are statistically significant at $P < 0.05$.

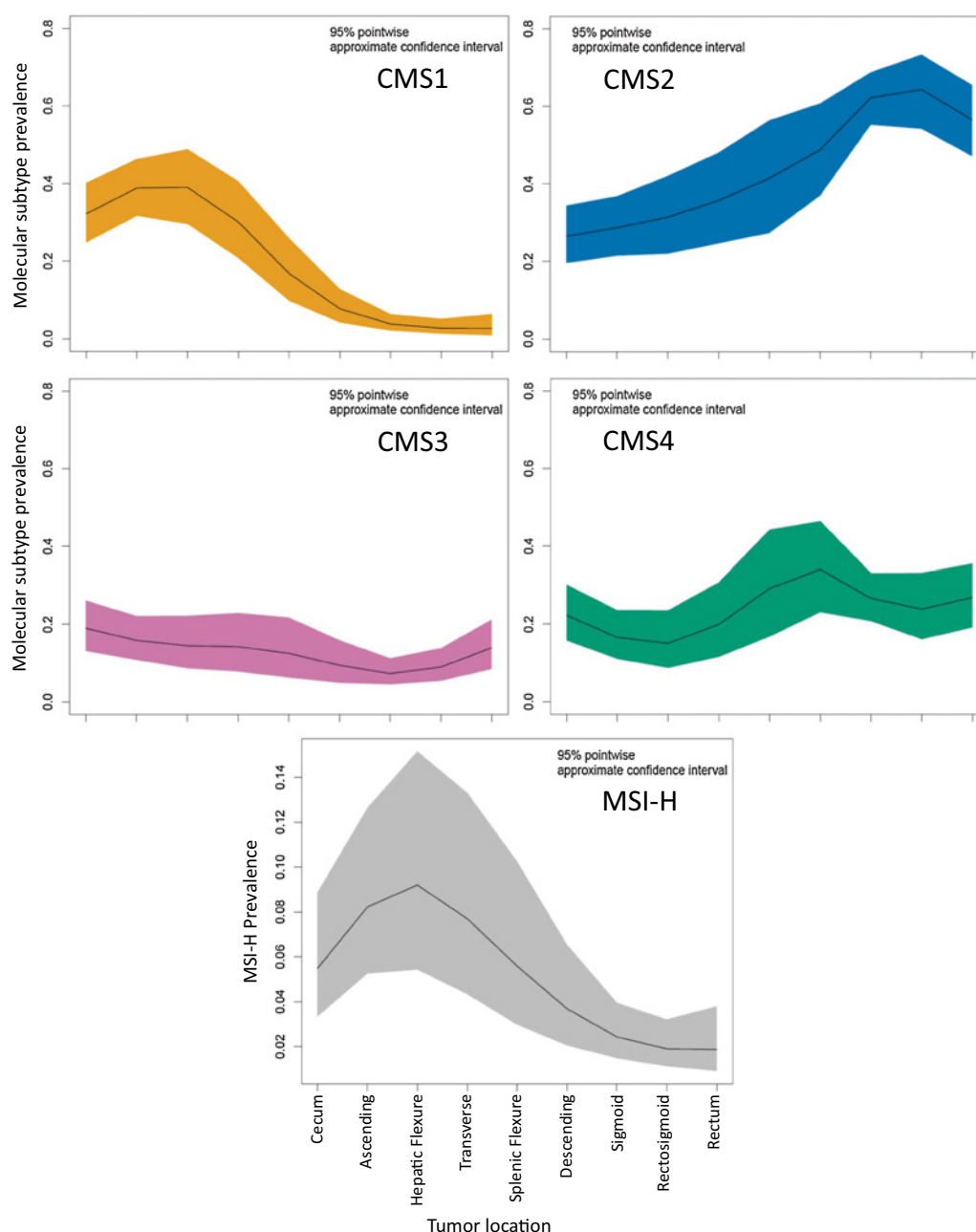
Only genes with a mutation in >10 patients in the cohort of 1,876 are displayed. Values in the table represent the number followed in parentheses by percentage.

accounted for by known covariates in a multivariate model but the remaining right-sided sites continued to be associated with a poor prognosis in the same model. We also assessed response rates to anti-EGFR therapy in patients with transverse tumors to see if they benefitted from these agents. As all patients in our study received their anti-EGFR agent in a second- or later line of therapy, the 181 trial of second-line FOLFIRI + panitumumab is the most reasonable trial for comparisons (7). In 181, treatment with FOLFIRI + panitumumab resulted in a progression-free survival of 8.0 months and a response rate of 49.7%. For right-sided tumors this was 4.8 months and 13.3%. Given the progression-free survival of 6.0 months and response rate of 39% among our heavily pretreated population, this would suggest that transverse tumors may still benefit from anti-EGFR agents. Taken together, these findings suggest that transverse tumors may be different from other traditionally right-sided locations.

Among left-sided sites, we also noted important characteristics that differed by location. For example, many descending colon features appear more "right sided." There was a higher proportion of mucinous histology in the descending colon (24%) compared with the sigmoid (14%), rectosigmoid junction (12%), or rectum (9%; $P = 0.0005$) and rates of *PIK3CA* ($P = 0.0009$) and *CTNNB1* ($P < 0.0001$) mutations were significantly higher than other left-sided locations. Mutation patterns noted in our study align well with a recent report by Marshall and colleagues demonstrating

significant differences between descending/splenic flexure tumors and those situated in the sigmoid or rectum (29). While not statistically associated with a worse OS than other left-sided tumors, there was also a trend toward worse outcomes (HR, 1.30; 95% CI, 0.93–1.80, $P = 0.12$) in the descending colon and Supplemental Figure 2S shows that there is considerable overlap in the HR estimates for all left/right divisions except when the rectosigmoid and rectal regions are considered separately. This suggests much of the differential survival effect for a right versus left comparison is driven by the rectosigmoid region. Our findings raise an interesting question as to whether the rectosigmoid region may be unique from the rest of the colon.

Despite highlighting mutational differences across similar sided locations, there are key oncogenic pathways that appear tumor side specific. The serrated pathway of colorectal carcinogenesis is characterized by mutations in *RAS/BRAF*, hypermethylation, frequently co-occurs with microsatellite instability and has a predilection for the right side (30). Though we noted rates of *RAS* mutations fall sharply from the cecum (70%) toward the ascending colon (57%) and hepatic flexure (43%), the total prevalence of a mutation in the MAP kinase pathway stays relatively stable due to a rising prevalence of *BRAF* mutations. By combining *BRAF* and *RAS* mutations, MAP kinase mutations are noted in 76% of cecal tumors, 82% of ascending colon, and much lower rates in the rest of the colon. Similarly, the *PIK3CA*–mTOR–AKT pathway has

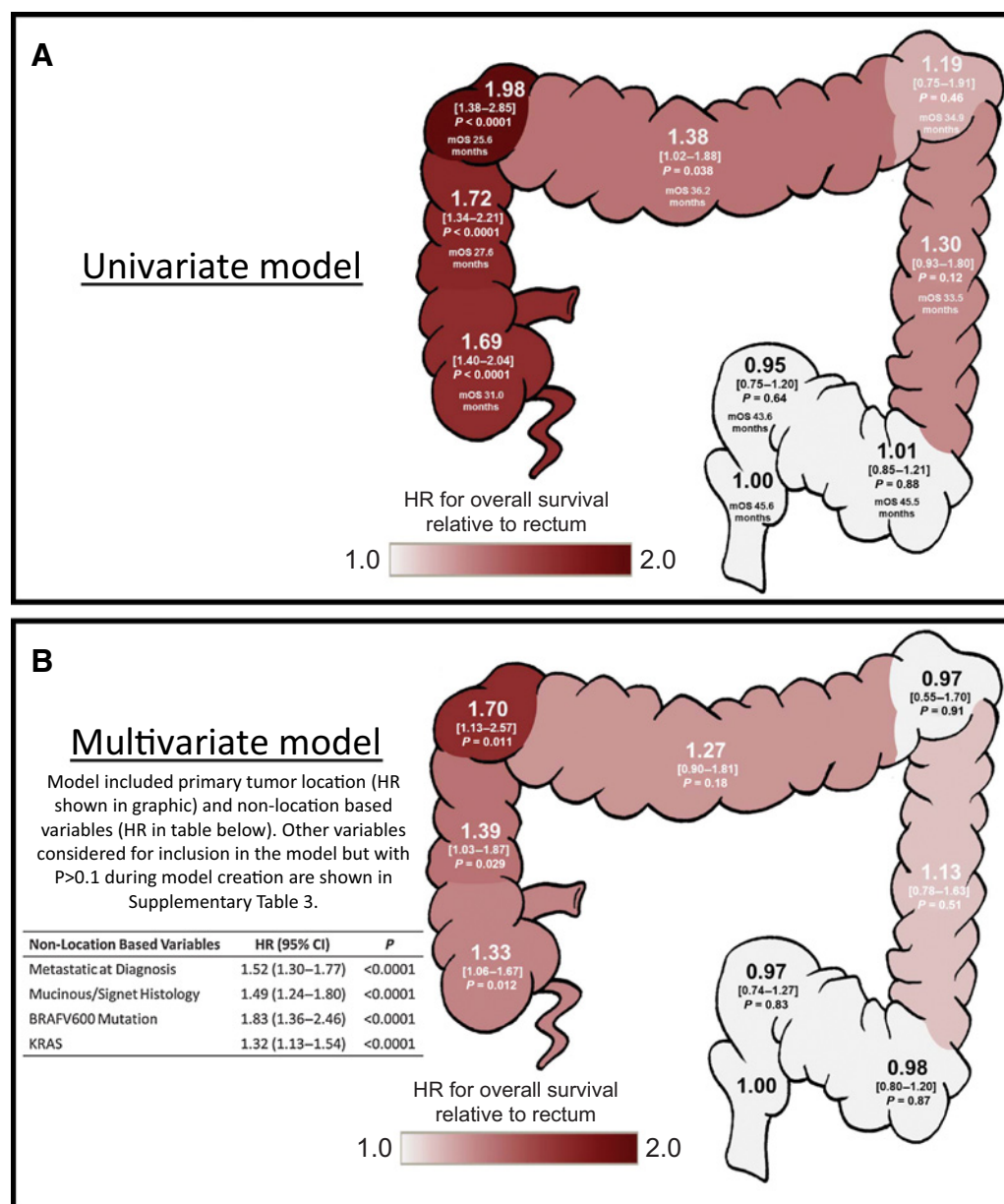
**Figure 3.**

Relative prevalence of consensus molecular subtypes at specific primary tumor locations. MSI-H, microsatellite instability high.

alterations that appear specific to the right side (4, 26, 27, 30, 31). The combination of *PIK3CA* and *PTEN* mutations is consistently present in 25% to 30% of all sites before falling to 16% in the sigmoid colon, 10% at the rectosigmoid junction, and 11% in the rectum. Though *PIK3CA* and *PTEN* mutation frequencies change across sites, their cumulative prevalence evens out so that combined pathway alterations are stable among tumor sites on the same side of the colon. These findings suggest that pathway alterations may be better conserved across similar sided locations than the individual alteration perturbing the pathway.

This biology of common canonical pathways is well characterized by the CMS subtypes that are based on gene expression analysis. The relative prevalence of each CMS subtype was similar in our study to the landmark paper that established its utility in colorectal cancer (4). In addition, the mutational profiles we noted in Fig. 1 appear consistent with hallmarks of the CMS subtypes. Specifically, we noted that the immune-driven CMS1 is most common in right-sided tumors and falls moving distally with an accompanying fall in MSI status and *BRAF* mutation rates. Similarly, we saw that the canonical CMS2 category rose moving

Loree et al.

**Figure 4.**

Comparison of overall survival based on primary tumor location in (A) a univariate model assessing only tumor location and (B) a multivariate proportional hazards model controlling for covariates that differed based on tumor location. Variables within the cartoon represent the hazard ratio for individual locations followed by the 95% confidence interval within square brackets.

from right to left, a trend that was accompanied by rising rates of *TP53* mutations. While our CMS subtype cohort is not matched to the main cohort of this study, it is useful to note that the pathways we noted as important from mutational analysis appear consistent with changing CMS prevalence by location. A further limitation of our CMS based results was that we were forced to pool metastatic and early-stage colorectal cancer patients for the CMS analysis due to a small number of stage IV patients with transcriptional profiling; however, others have shown that the proportion of each subtype is relatively stable between stages (4).

Our study has a number of other limitations that must be taken into account when interpreting results. The limited coverage of genes within our NGS assay did not allow assessment of copy-number changes that are important determinants of disease biology. As well, we relied on source document reports in order to assign tumor location. Given that these reports relied on endoscopic, pathologic, imaging, and clinical assessment of tumor location, we assume that they represent an accurate representation of location but there may be some cases where a tumor was on the boundary between two sites. However, given that the majority of our findings show a continuum of changes across the

bowel, small discrepancies in location likely caused little impact on the overall conclusions. We were also unable to incorporate treatment information for the entire cohort, which may have helped explain prognostic differences between locations.

Despite these weaknesses, our cohort had near-complete description of tumor location and presents one of the largest data sets analyzed for mutation differences by location. The size of this cohort is essential to ask what differentiates individual sites and provided significant power when looking at uncommon primary tumor locations such as the splenic or hepatic flexures. As well, the large size of our study enabled us to move beyond standard biomarkers like *RAS* and *BRAF* that have been well characterized and assess biomarkers representing "smaller pieces of the pie" that are becoming ever more important as we move into an era of precision medicine guided by molecular aberrations rather than histology alone.

Conclusion

In conclusion, we noted important differences in mutation prevalence between tumors located on the same side of the colon. Alterations in key pathways such as MAP kinase and PIK3CA–mTOR–AKT appeared stable across locations within the same side but important intra-side variances were noted. Specifically, the region from the sigmoid colon to the rectum appears unique and the transverse colon appears distinct from other right-sided locations.

Disclosure of Potential Conflicts of Interest

K. Raghav reports receiving speakers bureau honoraria from Bayer and Genentech. C. Eng reports receiving commercial research grants from Keryx/Daiichi, speakers bureau honoraria from Genentech, and is a consultant/advisory board member for Bayer/Sirtex. F. Meric-Bernstam reports receiving commercial research grants from Aileron, AstraZeneca, Bayer, Calithera, Curis, CytoMx, Debiopharma, eFFECTOR, Genentech, Jounce, Novartis, Pfizer, PUMA, Taiho, and Zymeworks; and is a consultant/advisory board member for Clearlight Diagnostics, Darwin Health, Dialecta, GRAIL, Inflection Bio-

sciences, Pieris, and Sumitomo Dainippon Pharma. D.M. Maru is a consultant/advisory board member for Bristol-Myers Squibb. No potential conflicts of interest were disclosed by the other authors.

Authors' Contributions

Conception and design: J.M. Loree, K. Shaw, S. Kopetz

Development of methodology: J.M. Loree, K. Shaw, J.S. Morris, S. Kopetz
Acquisition of data (provided animals, acquired and managed patients, provided facilities, etc.): J.M. Loree, K. Raghav, V.K. Morris, S. Advani, C. Eng, K. Shaw, R. Broaddus, M.J. Routbort, F. Meric-Bernstam, D. Maru, S. Kopetz
Analysis and interpretation of data (e.g., statistical analysis, biostatistics, computational analysis): J.M. Loree, A.A.L. Pereira, M. Lam, A.N. Willauer, K. Raghav, A. Dasari, S. Advani, R. Broaddus, M.J. Routbort, Y. Liu, J.S. Morris, F. Meric-Bernstam, M.J. Overman, S. Kopetz

Writing, review, and/or revision of the manuscript: J.M. Loree, A.A.L. Pereira, M. Lam, A.N. Willauer, K. Raghav, A. Dasari, V.K. Morris, S. Advani, D.G. Menter, C. Eng, R. Broaddus, J.S. Morris, R. Luthra, F. Meric-Bernstam, M.J. Overman, D. Maru, S. Kopetz

Administrative, technical, or material support (i.e., reporting or organizing data, constructing databases): J.M. Loree, A.N. Willauer, D.G. Menter, K. Shaw, D. Maru, S. Kopetz

Study supervision: S. Kopetz

Acknowledgments

J.M. Loree is a member of the UBC Clinician Investigator program and was the recipient of the CAMO 2016 Research Fellowship, the CCF of ASCO—J. Edward Mahoney Foundation Young Investigator Award, and the RCPSC Detweiler Fellowship. S. Kopetz is the recipient of NIH R01 grants that supported this research (CA 172670 and CA 187238). This research was performed in partial fulfillment of requirements for an M.S. degree from MD Anderson UTHealth GSBS. We thank Jeanne Manalo for her assistance with graphical design.

The costs of publication of this article were defrayed in part by the payment of page charges. This article must therefore be hereby marked *advertisement* in accordance with 18 U.S.C. Section 1734 solely to indicate this fact.

Received August 28, 2017; revised October 13, 2017; accepted November 15, 2017; published OnlineFirst November 27, 2017.

References

- Holch JW, Ricard I, Stintzing S, Modest DP, Heinemann V. The relevance of primary tumour location in patients with metastatic colorectal cancer: a meta-analysis of first-line clinical trials. *Eur J Cancer* 2017;70:87–98.
- Loupakis F, Yang D, Yau L, Feng S, Cremolini C, Zhang W, et al. Primary tumor location as a prognostic factor in metastatic colorectal cancer. *J Natl Cancer Inst* 2015;107:dju427.
- Tran B, Kopetz S, Tie J, Gibbs P, Jiang ZQ, Lieu CH, et al. Impact of BRAF mutation and microsatellite instability on the pattern of metastatic spread and prognosis in metastatic colorectal cancer. *Cancer* 2011;117:4623–32.
- Guinney J, Dienstmann R, Wang X, de Reyniès A, Schlicker A, Soneson C, et al. The consensus molecular subtypes of colorectal cancer. *Nat Med* 2015;21:1350–6.
- Cha Y, Kim K-J, Han S-W, Rhee YY, Bae JM, Wen X, et al. Adverse prognostic impact of the CpG island methylator phenotype in metastatic colorectal cancer. *Br J Cancer* 2016;115:164–71.
- Venderbosch S, Nagtegaal ID, Maughan TS, Smith CG, Cheadle JP, Fisher D, et al. Mismatch repair status and BRAF mutation status in metastatic colorectal cancer patients: a pooled analysis of the CAIRO, CAIRO2, COIN, and FOCUS studies. *Clin Cancer Res* 2014;20:5322–30.
- Arnold D, Lueza B, Douillard JY, Peeters M, Lenz HJ, Venook A, et al. Prognostic and predictive value of primary tumour side in patients with RAS wild-type metastatic colorectal cancer treated with chemotherapy and EGFR directed antibodies in six randomised trials. *Ann Oncol* 2017;28:1713–29.
- Loree JM, Kopetz S. Recent developments in the treatment of metastatic colorectal cancer. *Ther Adv Med Oncol* 2017;9:551–64.
- Van Cutsem E, Cervantes A, Adam R, Sobrero A, Van Krieken JH, Aderka D, et al. ESMO consensus guidelines for the management of patients with metastatic colorectal cancer. *Ann Oncol* 2016;27:1386–422.
- Boeckx N, Koukakis R, Beeck K, Kafatos G, Deschoolmeester V, Rolfo C, et al. Primary tumor sidedness impacts on prognosis and treatment outcome: results from three randomized studies of panitumumab plus chemotherapy versus chemotherapy or chemotherapy plus bevacizumab in 1st and 2nd line RAS/BRAF WT mCRC. *Ann Oncol* 2016;27:15–42. 89P.
- Venook A, Niedzwiecki D, Ou F, Sargent D, Innocenti F, Fruth B, et al. Impact of primary tumor location on Overall Survival and Progression Free Survival in patients with metastatic colorectal cancer: Analysis of all RAS wt subgroup on CALGB/SWOG 80405 (Alliance). *ICO 2016;34:Supplemental Abstract 3504*.
- Brule SY, Jonker DJ, Karapetis CS, O'Callaghan CJ, Moore MJ, Wong R, et al. Location of colon cancer (right-sided versus left-sided) as a prognostic factor and a predictor of benefit from cetuximab in NCIC CO.17. *Eur J Cancer* 2015;51:1405–14.
- Tejpar S, Stintzing S, Ciardiello F, Tabernero J, Van Cutsem E, Beier F, et al. Prognostic and predictive relevance of primary tumor location in patients with RAS wild-type metastatic colorectal cancer retrospective analyses of the CRYSTAL and FIRE-3 trials. *JAMA Oncol* 2016;E-pub ahead of print.
- Cancer Genome Atlas Network. Comprehensive molecular characterization of human colon and rectal cancer. *Nature* 2012;487:330–7.

Loree et al.

15. Sepulveda AR, Hamilton SR, Allegra CJ, Grody W, Cushman-Vokoun AM, Funkhouser WK, et al. Molecular biomarkers for the evaluation of colorectal cancer: guideline from the American Society for Clinical Pathology, College of American Pathologists, Association for Molecular Pathology, and the American Society of Clinical Oncology. *J Clin Oncol* 2017;35:1453–96.
16. Meric-Bernstam F, Brusco L, Shaw K, Horombe C, Kopetz S, Davies MA, et al. Feasibility of large-scale genomic testing to facilitate enrollment onto genomically matched clinical trials. *J Clin Oncol* 2015;33:2753–62.
17. Chaturvedi A, Green PE, Carroll JD. K-modes clustering. *J Classif* 2001;18:35–55.
18. Huang Z. Extensions to the k-means algorithm for clustering large data sets with categorical values. *Data Min Knowl Discov* 1998;2:283–304.
19. San OM, Huynh V-N, Nakamori Y. An alternative extension of the k-means algorithm for clustering categorical data. *Int J Appl Math Comput Sci* 2004;14:241–7.
20. Roever C, Raabe N, Luebke K, Ligges U, Szepannek G, Zentgraf M. kIAR: Classification and visualization 2014. Available from: <https://cran.r-project.org/web/packages/kIAR/index.html>
21. Wickham H. *Elegant Graphics for Data Analysis - ggplot2*. New York: Springer-Verlag; 2009. Available from: <https://cran.r-project.org/web/packages/ggplot2/citation.html>
22. Eisenhauer EA, Therasse P, Bogaerts J, Schwartz LH, Sargent D, Ford R, et al. New response evaluation criteria in solid tumours: revised RECIST guideline (version 1.1). *Eur J Cancer* 2009;45:228–47.
23. Zhang J, Zheng J, Yang Y, Lu J, Gao J, Lu T, et al. Molecular spectrum of KRAS, NRAS, BRAF and PIK3CA mutations in Chinese colorectal cancer patients: analysis of 1,110 cases. *Sci Rep* 2015;5:18678.
24. Yamauchi M, Morikawa T, Kuchiba A, Imamura Y, Qian ZR, Nishihara R, et al. Assessment of colorectal cancer molecular features along bowel subsites challenges the conception of distinct dichotomy of proximal versus distal colorectum. *Gut* 2012;61:847–54.
25. Takahashi Y, Sugai T, Habano W, Ishida K, Eizuka M, Otsuka K, et al. Molecular differences in the microsatellite stable phenotype between left-sided and right-sided colorectal cancer. *Int J Cancer* 2016;139:2493–501.
26. Albuquerque C, Baltazar C, Filipe B, Penha F, Pereira T, Smits R, et al. Colorectal cancers show distinct mutation spectra in members of the canonical WNT signaling pathway according to their anatomical location and type of genetic instability. *Genes Chromosomes Cancer* 2010;49:746–59.
27. Rosty C, Young JP, Walsh MD, Clendenning M, Sanderson K, Walters RJ, et al. PIK3CA activating mutation in colorectal carcinoma: associations with molecular features and survival. Ashktorab H, editor. *PLoS One* 2013;8:e65479.
28. Sarshekeh AM, Advani S, Overman MJ, Manyam G, Kee BK, Fogelman DR, et al. Association of SMAD4 mutation with patient demographics, tumor characteristics, and clinical outcomes in colorectal cancer. *PLoS One* 2017;12:e0173345.
29. Marshall J, Lenz H, Xiu J, Wafik E, Swensen J, El Ghazaly H, et al. Molecular variances between rectal and left-sided colon cancers. *J Clin Oncol* 2017;35:suppl 4S; abstract 522.
30. Bettington M, Walker N, Clouston A, Brown I, Leggett B, Whitehall V. The serrated pathway to colorectal carcinoma: current concepts and challenges. *Histopathology* 2013;62:367–86.
31. Lan Y-T, Jen-Kou L, Lin C-H, Yang S-H, Lin C-C, Wang H-S, et al. Mutations in the RAS and PI3K pathways are associated with metastatic location in colorectal cancers. *J Surg Oncol* 2015;111:905–10.

Clinical Cancer Research

Classifying Colorectal Cancer by Tumor Location Rather than Sidedness Highlights a Continuum in Mutation Profiles and Consensus Molecular Subtypes

Jonathan M. Loree, Allan A.L. Pereira, Michael Lam, et al.

Clin Cancer Res 2018;24:1062-1072. Published OnlineFirst November 27, 2017.

Updated version Access the most recent version of this article at:
doi:[10.1158/1078-0432.CCR-17-2484](https://doi.org/10.1158/1078-0432.CCR-17-2484)

Supplementary Material Access the most recent supplemental material at:
<http://clincancerres.aacrjournals.org/content/suppl/2017/11/23/1078-0432.CCR-17-2484.DC1>

Cited articles This article cites 26 articles, 3 of which you can access for free at:
<http://clincancerres.aacrjournals.org/content/24/5/1062.full#ref-list-1>

Citing articles This article has been cited by 1 HighWire-hosted articles. Access the articles at:
<http://clincancerres.aacrjournals.org/content/24/5/1062.full#related-urls>

E-mail alerts [Sign up to receive free email-alerts](#) related to this article or journal.

Reprints and Subscriptions To order reprints of this article or to subscribe to the journal, contact the AACR Publications Department at pubs@aacr.org.

Permissions To request permission to re-use all or part of this article, use this link
<http://clincancerres.aacrjournals.org/content/24/5/1062>.
Click on "Request Permissions" which will take you to the Copyright Clearance Center's (CCC) Rightslink site.